



Published in final edited form as:

J Immunol. 2008 November 1; 181(9): 5990–6001.

OX40 Costimulatory Signals Potentiate the Memory Commitment of Effector CD8⁺ T Cells

Seyed Fazlollah Mousavi^{*}, Pejman Soroosh^{2,*}, Takeshi Takahashi^{*}, Yasunobu Yoshikai[†], Hao Shen[‡], Leo Lefrançois[§], Jannie Borst[¶], Kazuo Sugamura^{*}, and Naoto Ishii^{*,3}

^{*}Department of Microbiology and Immunology, Tohoku University Graduate School of Medicine, Sendai, Japan [†]Division of Host Defense, Medical Institute of Bioregulation, Kyushu University, Fukuoka, Japan [‡]Department of Microbiology, University of Pennsylvania School of Medicine, Philadelphia, PA 19104 [§]Department of Immunology, University of Connecticut Health Center, Farmington, CT 06030 [¶]Division of Immunology, The Netherlands Cancer Institute, Amsterdam, The Netherlands

Abstract

A T cell costimulatory molecule, OX40, contributes to T cell expansion, survival, and cytokine production. Although several roles for OX40 in CD8⁺ T cell responses to tumors and viral infection have been shown, the precise function of these signals in the generation of memory CD8⁺ T cells remains to be elucidated. To address this, we examined the generation and maintenance of memory CD8⁺ T cells during infection with *Listeria monocytogenes* in the presence and absence of OX40 signaling. We used the expression of killer cell lectin-like receptor G1 (KLRG1), a recently reported marker, to distinguish between short-lived effector and memory precursor effector T cells (MPECs). Although OX40 was dispensable for the generation of effector T cells in general, the lack of OX40 signals significantly reduced the number and proportion of KLRG1^{low} MPECs, and, subsequently, markedly impaired the generation of memory CD8⁺ T cells. Moreover, memory T cells that were generated in the absence of OX40 signals in a host animal did not show self-renewal in a second host, suggesting that OX40 is important for the maintenance of memory T cells. Additional experiments making use of an inhibitory mAb against the OX40 ligand demonstrated that OX40 signals are essential during priming, not only for the survival of KLRG1^{low} MPECs, but also for their self-renewing ability, both of which contribute to the homeostasis of memory CD8⁺ T cells.

The adaptive immune responses to infection are mounted by the optimal differentiation of naive T and B cells into effector cells, and subsequently into long-lived memory cells. Memory CD8⁺ T cells represent the major effector arm of the adaptive immune system to maintain long-lived protective immunity against intracellular bacteria, protozoa, and viruses (1,2). Upon a subsequent infection by the same pathogen, pathogen-specific memory CD8⁺ T cells that have been maintained in the absence of Ag are poised to respond quickly, specifically, and with sufficient amplitude to protect the host (3–5). Therefore, understanding the mechanisms underlying the generation and maintenance of memory CD8⁺ T cells is critical, not only for contributing to basic immunology, but also for improved clinical applications, such as the design of new vaccines.

Copyright © 2008 by The American Association of Immunologists, Inc.

3Address correspondence and reprint requests to Dr. Naoto Ishii, Department of Microbiology and Immunology, Tohoku University Graduate School of Medicine, 2-1 Seiryomachi, Aoba-ku, Sendai 980-8575 Japan. ishiin@mail.tains.tohoku.ac.jp.

²Current address: Division of Molecular Immunology, La Jolla Institute for Allergy and Immunology, La Jolla, CA 92037.

Disclosures The authors have no financial conflict of interest.

Effector CD8⁺ T cells are phenotypically diverse, with different fates and memory potentials (6–10). To identify memory precursor cells from among the effector T cells, Kaech and colleagues (8) recently demonstrated, using acute viral infection models, that killer cell lectin-like receptor G1 (KLRG1)⁴ is a good marker for distinguishing between short-lived effector CD8⁺ T cells (KLRG1^{high}) and the memory precursor effector CD8⁺ T cells (MPECs; KLRG1^{low}). The same paper also demonstrated that long-lived CD8⁺ T cells that have the ability to homeostatically turn over have the KLRG1^{low} phenotype. In this study, we used this marker to examine the process of memory T cell generation, during which MPECs survive, expand, and finally differentiate into memory T cells.

Accumulating evidence shows that TCR signals and homeostatic cytokines, such as IL-7 and IL-15, are critical regulators of the generation and maintenance of CD8⁺ memory T cells (11,12). TCR signals are essential for the survival of naive T cells and the generation of functional memory T cells. Signals through the receptors for IL-7 and IL-15 of memory T cells have been well studied and shown to mediate not only the acute homeostatic proliferation of T cells, but also the basal homeostatic proliferation of memory T cells. The basal homeostatic proliferation mediates Ag-independent self-renewal of memory T cells in a full T cell environment (13,14). However, the roles played by costimulatory signals in the generation and maintenance of CD8⁺ memory T cells are still unclear. Among the T cell costimulatory molecules are several TNF receptor superfamily members, including OX40 (CD134), CD27, and 4-1BB, which contribute to the survival and expansion of effector T cells (15–22). Some of these T cells subsequently differentiate into long-lived memory T cells. The role of OX40 in the generation of memory CD4⁺ T cells has been intensively studied and convincingly demonstrated to be important (23,24). In addition, recent studies suggest that OX40 signals are also important for the generation of memory CD8⁺ T cells (19,25–27), although how and when OX40 signals are required remain to be elucidated.

In the present study, we took advantage of a useful model for acute bacterial infection. This model combines infection by recombinant *Listeria monocytogenes* expressing OVA (rLM-OVA) (28), which mimics the bacterial Ag during infection, with the MHC class I-restricted OVA-specific TCR-transgenic OT-I system (29). We also relied on the KLRG1^{low} phenotype as a specific marker for memory precursor T cells, which helped us to investigate the role of OX40 signals during infection, to determine when the effector CD8⁺ T cells undergo memory commitment. Finally, we used extensive adoptive transfer experiments to demonstrate the critical roles played by OX40 signals in both the generation and the maintenance of memory CD8⁺ T cells.

Materials and Methods

Mice

Six- to 8-wk-old female wild-type C57BL/6 mice were purchased from Japan SLC. OX40 ligand (OX40L)-deficient mice and Ly5.1⁺-C57BL/6 mice were previously described (21, 30,31). OT-I TCR-transgenic mice were a gift from W. Heath (Walter and Eliza Hall Institute, Melbourne, Australia) and were used as a source of CD8⁺ T cells specifically responsive to the OVA_{257–264} peptide (29). Ly5.1⁺ wild-type OT-I and Ly5.1⁺ OX40^{-/-} OT-I mice were generated in-house by intercrossing OT-I mice with Ly5.1⁺ wild-type and Ly5.1⁺ OX40^{-/-} mice, respectively. All of the mice were on a C57BL/6 background, and they were bred and maintained under specific pathogen-free conditions at Institute for Animal Experimentation, Tohoku University Graduate School of Medicine. All procedures were performed according

⁴Abbreviations used in this paper: KLRG1, killer cell lectin-like receptor G1; DC, dendritic cell; MPEC, memory precursor effector T cell; OX40L, OX40 ligand; rLM-OVA, recombinant *Listeria monocytogenes* expressing OVA.

to protocols approved by the Institutional Committee for the Use and Care of Laboratory Animals of Tohoku University.

Microorganism, immunization, and assessment of bacterial burden

rLM-OVA was previously described (28,32). Mice were infected via the tail vein with a sublethal dose of rLM-OVA (1×10^4 CFU; 0.1 LD₅₀) in 0.2 ml of PBS. To examine the protective function of memory T cells, the recipient mice that harbored long-lived wild-type or OX40^{-/-} OT-I cells were rechallenged with a higher dose of rLM-OVA (1×10^5 CFU). To evaluate the bacterial burden, the spleen and liver were removed and separately homogenized in 3 ml of PBS. Serial dilutions of each tissue extract were spread on Brain-Heart Infusion agar plates containing erythromycin, and the number of colonies was counted after incubation for 24–48 h at 37°C.

Antibodies

The following Abs and reagents were purchased from BD Biosciences: anti-CD8 allophycocyanin, anti-TCR V α 2-PE, anti-TCR V β 5-FITC, anti-Ly5.1 biotin, anti-Ly5.1 allophycocyanin, anti-CD11b FITC, anti-CD11c PE, anti-CD44 PE, anti-CD62L FITC, anti-CD62L biotin, anti-OX40 biotin, anti-granzyme B-PE, anti-IL-2 PE, anti-IFN- γ PE, streptavidin-allophycocyanin, and annexin V-FITC. Anti-mouse KLRG1 allophycocyanin was purchased from eBioscience. The inhibitory anti-OX40L mAb (MGP34; rat IgG2c) was previously described (21,33). The anti-IL-7R α -chain mAb (A7R34; rat IgG2a) was a gift from S. Nishikawa (Center for Developmental Biology, RIKEN, Kobe, Japan). Control rat Ig was purchased from Cappel. For staining OX40L and IL-7R α , MGP34 and A7R34 were biotinylated and visualized using streptavidin-allophycocyanin.

Lymphocyte isolation, cell sorting, and adoptive transfer

Naive CD8⁺ T cells (1×10^4) were purified from the spleen of Ag-naive wild-type OT-I or OX40^{-/-} OT-I mice with the Ly5.1⁺ congenic marker. They were then injected into the lateral tail vein of naive Ly5.2⁺ congenic mice that were infected with rLM-OVA 24 h after the cell transfer (first host). In some experiments, to block the OX40-OX40L interaction, the recipient mice were given control rat IgG (300 μ g) or blocking anti-OX40L mAb (MGP34) (300 μ g) by i.p. injection 1 day before, and on days 1, 3, 5, and 7 after the infection. For the secondary adoptive transfer of effector T cells, the Ly5.1⁺ effector donor cells were isolated from the spleen of the first host (Ly5.2⁺) 6 days after the rLM-OVA infection by adding biotinylated anti-Ly5.1 mAb, followed by anti-biotin MicroBeads (Miltenyi Biotec) and sorting on an AutoMACS cell sorter (Miltenyi Biotec). The enriched Ly5.1⁺ donor cells were further separated by a FACSAria cell sorter (Nippon BD) to purify KLRG1^{low}TCR-V α 2⁺CD8⁺ and KLRG1^{high}TCR-V α 2⁺CD8⁺ effector T cells. These cells (2×10^6 each), from the first host, which harbored either the wild-type OT-I or OX40^{-/-} OT-I donor cells, were adoptively transferred into an Ly5.2⁺ second host (wild-type mouse) that had been infected with wild-type *L. monocytogenes* 6 days previously to prepare an appropriate physiological environment for the effector donor cells. For another secondary transfer of memory T cells, Ly5.1⁺ memory donor cells were isolated 40 days after infection, as described above, and labeled with CFSE (Molecular Probes), as described previously (34,35). The CFSE-labeled memory T cells (1×10^6) that had been generated in the first host were transferred into a nonirradiated (wild type or OX40L deficient).

Flow cytometry analysis and intracellular staining

Before being stained, the cells were washed and resuspended in a staining buffer consisting of 1 \times PBS, 2% BSA, and 0.01% NaN₃. To block non-specific staining, the 2.4G2 anti-CD16/32 mAb was added. Abs for cell surface markers were added, and cells were incubated for 30 min

on ice. For intracellular cytokine staining, whole splenocytes (5×10^5) were stimulated with the OVA₂₅₇₋₂₆₄ peptide for 4 h in the presence of brefeldin A (10 μ g/ml; Invitrogen). Surface staining was performed with the indicated fluorochrome-conjugated mAbs. The cells were then resuspended in fixation/permeabilization solution (BD Cytofix/Cytoperm kit; BD Biosciences), and intracellular cytokine staining was performed according to the manufacturer's protocol. For intracellular staining of granzyme B, whole splenocytes were stained with Ly5.1 FITC and washed with chilled PBS. The cells were resuspended in the fixation/permeabilization solution (BD Cytofix/Cytoperm kit; BD Biosciences), and intracellular staining of granzyme B was performed, as described above. The samples were analyzed with a FACSCalibur flow cytometer (BD Immunocytometry Systems). The analyses were conducted using the CellQuest program (BD Immunocytometry Systems).

Determination of apoptosis

Whole splenocytes (5×10^5) that included effector donor T cells were cultured for 8 h in a complete medium (RPMI 1640 containing 10% FCS). The cells were then harvested and stained with anti-Ly5.1 mAb, anti-KLRG1 mAb, annexin V, and propidium iodide, according to the manufacturer's instructions. The intensity of the annexin V staining on the Ly5.1-gated cells was measured with a FACSCalibur flow cytometer.

Measurement of cytolytic activity

Splenocytes from recipient mice ($n = 3$ each) that possessed wild-type or OX40^{-/-} effector OT-I cells were collected 10 days after the infection. The cells collected (effector cells) were cocultured with ⁵¹Cr-labeled EL-4 cells (4×10^4) (target cells) at the indicated ratios in the presence (10 μ g/ml) or absence of OVA₂₅₇₋₂₆₄ peptide for 6 h. After the incubation, the radioactivities of the supernatants were determined with a γ counter. The results are expressed as the percentage of specific lysis = ((release in test – spontaneous release)/(release by detergent – spontaneous release)) \times 100.

Statistical analysis

Statistical analyses were performed with Student's *t* test. Values of $p < 0.01$ were considered significant. * and ** in any graph represent $p < 0.01$ and $p < 0.001$, respectively.

Results

Expression of OX40 and OX40L during *Listeria* infection

OX40 is transiently expressed on activated T cells upon antigenic stimulation, and its ligand, OX40L, is induced on mature APCs and activated T cells (19,21,35,36). To address when OX40 and OX40L interact during *Listeria* infection, we examined their expression profiles on CD8⁺ T cells from OVA-specific TCR-transgenic (OT-I) mice. Naive Ly5.1⁺ OT-I T cells were adoptively transferred into congenic Ly5.2⁺ wild-type mice, followed by immunization with a sublethal dose of *rLM*-OVA. At various time points after the infection, the expression of OX40 and OX40L on donor T cells and recipient APCs, respectively, was examined. Although naive donor CD8⁺ T cells did not express OX40, its expression was induced on activated donor T cells on day 2, peaked on day 3, and had become undetectable again by day 10 after the infection (*left*, Fig. 1). OX40L expression on several types of APCs, including CD11b⁺CD11c⁻ macrophages, CD11b⁺CD11c⁺ myeloid dendritic cells (DCs), and CD11b⁻CD11c⁺ lymphoid DCs, was also investigated. OX40L was transiently expressed on myeloid DCs, but not on macrophages or lymphoid DCs during *Listeria* infection (Fig. 1). Although in vitro activated CD4⁺ T cells express OX40L (35), OX40L expression on donor CD8⁺ T cells could not be detected at any time during the *Listeria* infection (data not shown).

These data suggest that OX40 signals were provided through T cell-myeloid DC interactions during the acute phase of the *Listeria* infection.

OX40 signals are dispensable for the expansion and function of activated CD8⁺ T cells, but determine the number of the KLRG1^{low} MPEC population

OX40 signals are not essential for the initial proliferation of CD4⁺ T cells during the priming phase of Ag stimulation, but significantly promote the survival and clonal expansion of effector CD4⁺ T cells in the later effector phase (16,22,30). To examine whether OX40 might have a similar function in CD8⁺ T cell responses, naive wild-type and OX40^{-/-} OT-I CD8⁺ T cells were adoptively transferred into congenic wild-type mice that were subsequently immunized with a sub-lethal dose of *rLM-OVA*. The recipient mice harboring wild-type and OX40^{-/-} donor cells showed a similar kinetics of bacterial burdens after *rLM-OVA* infection, and cleared the bacteria equally well from the spleen and liver by day 6 postinfection (Fig. 2A). This suggests that both wild-type and OX40^{-/-} donor cells were activated and differentiated under a similar inflammatory environment mediated by *Listeria* infection. At various time points postinfection, the donor cells were recovered from the spleens of the recipient mice. Both wild-type and OX40^{-/-} OT-I donor cells could be detected in the spleen on day 2 after the infection, reached their peak number on day 6, and declined thereafter (Fig. 2B), much as described for CD4⁺ T cells. The cytotoxic activity of spleen cells derived from recipient mice harboring OX40-KO OT-I donor cells was comparable to that of spleen cells derived from recipient mice harboring wild-type donor cells (Fig. 2C). Although previous reports demonstrated that OX40 signals enhanced granzyme B expression in effector CD8⁺ T cells (25), Fig. 2D shows that wild-type and OX40^{-/-} donor cells produced a comparable amount of granzyme B. Furthermore, these results indicate that the OX40 signals are dispensable for the expansion and function of activated CD8⁺ T cells during the acute phase of infection.

To investigate the phenotypic heterogeneity of the effector CD8⁺ T cell population, we used KLRG1 expression to distinguish between short-lived effector cells (KLRG1^{high}) and MPECs (KLRG1^{low}) (6,8), as well as the expression of the IL-7R α -chain (IL-7R) (high on MPECs) and CD62L. Flow cytometric analysis gated on KLRG1 expression at various time points after infection revealed phenotypic heterogeneity in the wild-type and OX40^{-/-} effector T cells in the spleen. Six days after *Listeria* infection, effector CD8⁺ T cells differentiated into the two distinct cell lineages, KLRG1^{high} and KLRG1^{low}, in which the KLRG1^{low} (IL-7R^{high}) population was expected to contain memory precursors (8). Although the total donor cell numbers in recipient mice harboring wild-type or OX40^{-/-} OT-I cells were comparable even 10 days after infection, the subpopulation profiles were quite different in terms of KLRG1 expression. In particular, the percentage and the absolute number of KLRG1^{low} MPECs in the OX40^{-/-} OT-I cells were markedly lower than in the wild-type OT-I cells (Fig. 2, E and F). Compatible with a previous paper (8), almost all KLRG1^{low} cells had the IL-7R^{high} phenotype; we found that this was true regardless of OX40 signaling (Fig. 2E).

Because a recent report demonstrated that KLRG1^{high} effector T cells more efficiently produce IFN- γ than KLRG1^{low} effector T cells during viral infection (8), we further examined cytokine production of these effector T cells during *Listeria* infection. Unexpectedly, ex vivo Ag stimulation of KLRG1^{high} and KLRG1^{low} effector T cells from a 10-day infected recipient showed similar levels of their IFN- γ production even in the absence of OX40 signals. In contrast, a smaller population (25%) in OX40^{-/-} KLRG1^{low} T cells produced IL-2 compared with that (55%) in wild-type KLRG1^{low} effector T cells (Fig. 2G), suggesting that OX40 signals promote IL-2 synthesis by MPECs. Similar results were found 8 days after infection (data not shown). Furthermore, flow cytometric analyses did not show significant differences in the expression profiles for other effector/differentiation markers, such as CD25, CD27, CD43, and CD44, between wild-type and OX40^{-/-} OT-I donor cells (data not shown).

Collectively, these observations suggest that OX40 signals are necessary for the optimal generation of KLRG1^{low}CD8⁺ MPECs, despite their dispensability for the effector function of activated CD8⁺ T cells.

OX40 signals are essential for the generation of functional memory CD8⁺ T cells

We next assessed the accumulation of long-lived OT-I donor cells in the spleens of infected mice at the memory phase. Approximately 2-fold more wild-type OT-I donor cells had accumulated than OX40^{-/-} OT-I cells on day 30 (Fig. 3A). Intriguingly, on day 60 and until day 150 after infection, the number of persisting OX40^{-/-} donor T cells in the spleen was markedly reduced compared with wild-type donor T cells (Fig. 3A). There were also many fewer OX40^{-/-} donor cells in the liver and bone marrow of recipient mice on day 150 than wild-type donor cells in these tissues (Fig. 3B). These results suggest that OX40 critically contributes to the generation and probably the maintenance of memory CD8⁺ T cells.

Phenotypic analysis of the persisting donor cells on day 90 demonstrated that wild-type donor cells were predominantly KLRG1^{low} IL-7R^{high}CD62L^{high} (Fig. 3C). In contrast, in the absence of OX40, a substantial percentage of the IL-7R^{high}CD62L^{high} donor CD8⁺ T cells strongly expressed KLRG1, indicating that the majority of long-lived OX40^{-/-} donor T cells was unable to acquire the memory phenotype (Fig. 3C). In addition, consistent with a previous report (37,38), these data imply that a high expression of IL-7R on OX40^{-/-} OT-I cells is not sufficient to support their survival.

One of the cardinal properties of memory CD8⁺ T cells is their ability to protect the host against secondary infection. To address whether the persisting CD8⁺ T cells that were generated in the absence of OX40 signals are protective, 90 days after the first infection, the recipient mice that had harbored long-lived wild-type or OX40-KO OT-I donor cells were infected with a higher dose of rLM-OVA. As expected, recipient mice possessing the long-lived wild-type OT-I donor cells completely cleared the bacteria from their spleens by day 3 after reinfection (Fig. 3D). In comparison, mice harboring persisting OX40^{-/-} OT-I cells were not able to clear bacteria from the spleen, and had 100,000-fold more bacteria in the liver (Fig. 3D). Because the impaired protection seen in the OX40^{-/-} donor cell recipients correlated with the reduced number of functional memory T cells (Fig. 3E), we compared the *in vivo* protective function between wild-type and OX40^{-/-} memory T cells. The equal number of long-lived wild-type and OX40^{-/-} donor T cells was collected from the first hosts, and transferred into the naive second hosts. Even the second host receiving the OX40^{-/-} memory donor cells showed no weight loss after infection with a lethal dose of rLM-OVA (data not shown). Bacterial clearance from the spleen of the two different second hosts was similar (Fig. 3F), suggesting the comparable protective function between wild-type and OX40^{-/-} memory T cells generated in the first host.

Next, the functionality of long-lived wild-type and OX40^{-/-} OT-I cells during *in vitro* recall responses was examined. Ninety days postinfection, whole splenocytes from each recipient mouse were collected and stimulated with OVA₂₅₇₋₂₆₄ peptide, and the synthesis of IL-2 and IFN- γ was analyzed by intracellular staining. Long-lived OX40^{-/-} OT-I donor cells, especially the KLRG1^{low} population, failed to produce IL-2, whereas wild-type memory CD8⁺ T cells secreted substantial amounts of IL-2; both kinds of donor cells produced IFN- γ at the same level, regardless of KLRG1 expression (Fig. 3G). In addition, 60% of wild-type KLRG1^{low} cells produced IL-2, whereas only 34% of OX40^{-/-} KLRG1^{low} population was positive for IL-2, suggesting the importance of OX40 in IL-2 secretion by each KLRG1^{low} T cell. The absolute number of IL-2-producing KLRG1^{low} cells derived from OX40^{-/-} OT-I cells *in vitro* was also markedly reduced (Fig. 3G).

OX40 signals contribute to the survival of KLRG1^{low} memory precursor cells

Several previous papers have suggested that OX40 signals promote the survival of effector CD4⁺ and CD8⁺ T cells, probably leading to the effective generation of memory T cells. To elucidate the mechanisms for the OX40-mediated generation of memory CD8⁺ T cells, we examined the susceptibility to apoptosis of effector CD8⁺ T cells collected from the recipient mice 6 days after infection. Interestingly, half of the KLRG1^{low} population in the OX40^{-/-} effector CD8⁺ T cells became apoptotic after only 8 h in complete medium, whereas almost all of the wild-type KLRG1^{low} effector CD8⁺ T cells remained alive (Fig. 4A), indicating an increased susceptibility of OX40^{-/-} MPECs to apoptosis. In contrast to the MPEC population, the KLRG1^{high} effector population did not show substantial apoptosis, even in the absence of OX40 signals (Fig. 4A).

To clarify the significance of the OX40-mediated survival of KLRG1^{low} MPECs, we compared the process of memory T cell generation from purified KLRG1^{high} and KLRG1^{low} effector CD8⁺ T cells in the presence or absence of OX40 signals. Equal numbers of isolated KLRG1^{high} and KLRG1^{low} effector CD8⁺ T cells that were generated in the first host (harboring either wild-type or OX40-KO donor OT-I cells), during the 6 days following infection, were independently transferred into second recipients that had been infected with *Listeria* 6 days previously. The accumulation of donor cells in the spleen of the second recipients was assessed 7, 20, and 60 days after the transfer. As expected, the absolute number of persisting cells was greater on day 7 after the transfer of wild-type KLRG1^{low} effector CD8⁺ T cells than after the transfer of KLRG1^{high} effector CD8⁺ cells, and this difference was still observed on day 60 posttransfer (Fig. 4B). In addition, the transferred KLRG1^{high} population from both wild-type and OX40^{-/-} OT-I cells remained mainly KLRG1^{high}, whereas both KLRG1^{high} and KLRG1^{low} long-lived cells were observed when KLRG1^{low} effector CD8⁺ T cells were transferred (Fig. 4C), indicating that the KLRG1^{low} effector CD8⁺ T cells may give rise to both sets of cells. Notably, by day 60, no donor cells derived from the OX40^{-/-} MPECs could be found (Fig. 4, B and C), indicating that OX40 signals play a critical role in the survival of KLRG1^{low} MPECs.

OX40 is essential for the self-renewal potential of memory CD8⁺ T cells

Although the more rapid reduction of MPECs in OX40^{-/-} T cells during the contraction phase is one of the possible mechanisms for the failure of OX40^{-/-} donor cells to generate memory T cells, it cannot fully explain their decrease after the contraction phase (between days 60 and 150 in Fig. 3A). Therefore, we postulated that OX40 might also be implicated in the maintenance of memory T cells. Because the basal homeostatic proliferation contributes to the maintenance of memory CD8⁺ T cells by mediating their Ag-independent self-renewal (8,13,14), we have addressed whether OX40 might be involved in the basal homeostatic proliferation. Wild-type memory OT-I or OX40^{-/-} memory OT-I cell populations from the first host were isolated, labeled with CFSE, and then adoptively transferred into Ag-naive wild-type second hosts. Although the KLRG1 expression profiles between wild-type and OX40^{-/-} memory donor cells were different, their IL-7R expression levels were comparable (Fig. 5A). The basal homeostatic proliferation of these memory CD8⁺ T cells was assessed by the dilution of CFSE intensity 30 days after transfer. When wild-type OT-I memory CD8⁺ T cells were transferred, the KLRG1^{low} population divided between one and four times, but most of the KLRG1^{high} cells appeared to stop after one division (Fig. 5B). The significantly greater self-renewal potential of the KLRG1^{low} long-lived CD8⁺ T cells is concordant with their being memory CD8⁺ T cells, which is consistent with the findings for viral infection. In striking contrast, long-lived KLRG1^{low} OX40^{-/-} donor cells failed to undergo homeostatic proliferation, and their KLRG1^{high} population almost disappeared (Fig. 5B). Furthermore, the absolute number of long-lived OX40^{-/-} donor cells in the second host was much lower than that of wild-type donor cells (Fig. 5B). These data indicate that OX40 signals critically mediate the basal

homeostatic proliferation of memory CD8⁺ T cells, especially KLRG1^{low} memory CD8⁺ T cells.

We next addressed whether OX40 signals during the memory phase are responsible for the self-renewal of memory T cells. Persisting wild-type OT-I donor cells were isolated from the first host 40 days after infection, and adoptively transferred into an Ag-naive wild-type or OX40L-deficient second host. In contrast to the OX40^{-/-} long-lived CD8⁺ T cells, which could not divide, wild-type memory OT-I cells in the OX40L-deficient host exhibited a robust homeostatic proliferation and similar cell accumulation as in the wild-type host (Fig. 5C). These transfer experiments imply that OX40 signals are not essential during the memory phase for the self-renewal of memory CD8⁺ T cells, which may be programmed by previously provided OX40 signals.

OX40 signals during priming are responsible for the generation and maintenance of memory CD8⁺ T cells

As shown in Fig. 1, it is likely that OX40 and OX40L interactions occur through T cell-APC interactions at the T cell priming phase during *Listeria* infection. Given the dispensability of OX40 signals during the memory phase for memory T cell self-renewal (Fig. 5B), OX40 signals during priming thus might be essential and sufficient for the generation and maintenance of memory CD8⁺ T cells. To address this possibility, we administered a blocking anti-OX40L mAb to recipient mice, during only the initial 7 days after the rLM-OVA infection, and the accumulation of donor cells in the spleen of the recipient mice was assessed. Similar to the initial expansion of the OX40^{-/-} T cells (Fig. 2B), treatment with the anti-OX40L mAb did not have any effect on the expansion of OT-I donor cells during the priming and effector phases (Fig. 6A), confirming that OX40 signals are not crucial for the generation of Ag-specific effector CD8⁺ T cells. However, as expected, the accumulation of long-lived OT-I donor cells in anti-OX40L mAb-treated mice was dramatically reduced (~4% of the level in control IgG-treated hosts on day 90) (Fig. 6A), and the kinetics for the decrease in the persisting donor cell number was similar to that of the OX40^{-/-} donor cells (Fig. 2B). Anti-OX40L mAb treatment also suppressed the generation of KLRG1^{low}IL-7R^{high}CD62L^{high} memory CD8⁺ T cells (Fig. 6C). Furthermore, the KLRG1^{low} memory subset of donor cells that had been generated in the host treated with the anti-OX40L mAb failed to produce IL-2 upon ex vivo Ag restimulation (Fig. 6D). These results were very similar to those obtained using OX40^{-/-} donor cells.

Finally, to investigate whether blocking OX40 signals only during priming could suppress the self-renewal of memory CD8⁺ T cells, long-lived wild-type OT-I donor cells were isolated from a first host that had been treated with inhibitory anti-OX40L mAb or control IgG during the priming phase of the *Listeria* infection, labeled with CFSE, and then adoptively transferred into Ag-naive wild-type second hosts. Similar to the defective self-renewal of the OX40^{-/-} memory T cells (Fig. 5A), the long-lived OT-I donor cells derived from effector CD8⁺ T cells generated in the absence of OX40 signals failed to show homeostatic proliferation in the second host (Fig. 6E). These results not only confirm that OX40 signals are required for the generation of KLRG1^{low} memory CD8⁺ T cells, but also suggest that OX40 signals are essential during priming for the self-renewal of memory CD8⁺ T cells.

Discussion

Recent findings have clearly demonstrated that effector CD8⁺ T cells are phenotypically diverse in terms of KLRG1 expression (6,7), and indicate that KLRG1^{low} effector CD8⁺ T cells become committed to the memory fate during acute viral infection (8–10). The present study has confirmed these observations in an acute bacterial infection model and further obtained several new findings on the OX40 roles in the homeostasis of KLRG1^{low} effector and memory T cells. With regard to the OX40 signals' roles in the generation and homeostasis of

memory CD8⁺ T cells, several previous papers have suggested OX40 to be important for the survival of heterogeneous effector CD8⁺ T cells (19,25–27). The present results demonstrate that OX40 signals promote the survival of KLRG1^{low} CD8⁺ MPECs, a subset of effector T cells. Because OX40 stimulation directly induces NF-κB-associated survival signals in activated T cells (23,24,39), the NF-κB activation may be involved in the OX40-mediated survival of KLRG1^{low} CD8⁺ MPECs.

We also show in this study that OX40 signals critically potentiated the maintenance of the memory CD8⁺ T cells. Furthermore, the OX40 signals activated during priming appeared to be sufficient to imprint the self-renewal potential of KLRG1^{low} memory CD8⁺ T cells onto the MPECs (Figs. 5B and 6E). In addition, we previously demonstrated using an acute viral infection model that OX40 signals during Ag priming are required for the expansion of memory CD8⁺ T cells during secondary infection (19). Therefore, OX40 signals during priming seem to imprint the memory competency onto CD8⁺ MPECs. The OX40-mediated memory imprinting may indicate a novel role for T cell costimulatory signals apart from the conventional survival signals. However, the question of how OX40 signals imprint the commitment for self-renewal onto CD8⁺ T cells that are Ag specifically activated remains unsolved. Our next study will therefore focus on the identification of the molecule(s) responsible for OX40-induced memory imprinting.

A higher proportion of KLRG1^{high} cells in the first host was observed in OX40^{-/-} donor cells than in wild-type donor cells in any time points during both the effector and the memory phases. However, KLRG1^{high} long-lived cells from OX40^{-/-} memory T cells were diminished when memory OX40^{-/-} T cells, which initially consisted of both KLRG1^{high} and KLRG1^{low} populations, were transferred into Ag-naive second hosts (Fig. 5B). Therefore, a certain environment in the first host after *Listeria* infection might be important to maintain the OX40^{-/-} KLRG1^{high} long-lived T cells, although the maintenance of the wild-type KLRG1^{high} long-lived T cells may not require the putative environment (Fig. 5B). A recent report suggests that KLRG1^{high} effector T cells may be specifically induced by inflammatory signals (i.e., IL-12) (8). Therefore, inflammation-mediated environments induced by *Listeria* infection in the first host may be essential for survival and generation of KLRG1^{high} CD8⁺ T cells from OX40^{-/-} donor T cells.

The deficiency of the OX40^{-/-} donor T cells in survival and self-renewal may be owing to some abnormality in unidentified endogenous factors, because the circumstances for memory generation and maintenance in the recipient (such as the lymph node structure, CD4⁺ T cells, APCs, stromal cells, and probably stromal cytokines, IL-7 and IL-15) were the same for wild-type and OX40^{-/-} donor cells in our experimental setting. We examined the donor cell expression of receptors for the homeostatic cytokines IL-7 and IL-15, which are expressed by recipient cells, because these cytokines mediate the homeostatic proliferation of memory T cells. However, IL-7R and CD122 (the shared β subunit for IL-2Rs and IL-15Rs) levels on the KLRG1^{low} population of OX40^{-/-} CD8⁺ T cells were similar to those on the KLRG1^{low} population of wild-type CD8⁺ T cells (Figs. 2E,3C, and 5A, and data not shown). In addition, the in vitro culture of activated OX40^{-/-} OT-I T cells showed a robust proliferative response to exogenous IL-2 (data not shown), suggesting that a lack of signaling molecules involved in the γc/JAK3/STAT pathway may not cause their impaired survival and self-renewal, and indicating that defective IL-7 and IL-15 signals are probably not associated with the impaired generation and maintenance of CD8⁺ T cells. We nevertheless found that KLRG1^{low} long-lived T cells are the main producer of IL-2, and that the IL-2 production by KLRG1^{low} MPECs and memory T cells that were generated in the absence of OX40 signals was severely impaired (Figs. 2G and 3G).

IL-2 is a well-known T cell-derived cytokine, which also controls several T cell responses, including their activation, expansion, and activation-induced cell death, and the generation of functional memory CD8⁺ T cells, in an autocrine or paracrine manner. IL-2 thus might be a key factor for the OX40-mediated survival of MPECs and maintenance of memory CD8⁺ T cells. This scenario is partially supported by a recent report showing that IL-2 signals during priming imprint functional memory properties onto CD8⁺ T cells, although the same paper also demonstrated that IL-2 is dispensable for the generation of long-lived CD8⁺ T cells (40). Based on this scenario, the ability of memory precursor and memory CD8⁺ T cells to produce IL-2 might be conferred on activated CD8⁺ T cells by OX40 signals during Ag priming. A precise understanding of OX40-mediated memory imprinting may provide us not only with important insights into the mechanisms of the development and homeostasis of memory T cells, but also with beneficial information for designing new vaccination strategies.

Acknowledgments

We thank Dr. K. Murata and R. Ito for the excellent technique, and S. Otake for critical help with infection experiments.

This work was supported in part by a grant-in-aid for scientific research on priority areas from the Ministry of Education, Culture, Sports, Science, and Technology of Japan and a grant-in-aid for scientific research on priority areas from the Japan Society for the Promotion of Science.

References

- Ahmed R, Gray D. Immunological memory and protective immunity: understanding their relation. *Science* 1996;272:54–60. [PubMed: 8600537]
- Williams MA, Holmes BJ, Sun JC, Bevan MJ. Developing and maintaining protective CD8⁺ memory T cells. *Immunol. Rev* 2006;211:146–153. [PubMed: 16824124]
- Rocha B, Tanchot C. CD8 T cell memory. *Semin. Immunol* 2004;16:305–314. [PubMed: 15528075]
- Veiga-Fernandes H, Walter U, Bourgeois C, McLean A, Rocha B. Response of naive and memory CD8⁺ T cells to antigen stimulation in vivo. *Nat. Immunol* 2000;1:47–53. [PubMed: 10881174]
- Lau LL, Jamieson BD, Somasundaram T, Ahmed R. Cytotoxic T-cell memory without antigen. *Nature* 1994;369:648–652. [PubMed: 7516038]
- Voehringer D, Blaser C, Brawand P, Raulet DH, Hanke T, Pircher H. Viral infections induce abundant numbers of senescent CD8 T cells. *J. Immunol* 2001;167:4838–4843. [PubMed: 11673487]
- Beyersdorf NB, Ding X, Karp K, Hanke T. Expression of inhibitory “killer cell lectin-like receptor G₁” identifies unique subpopulations of effector and memory CD8 T cells. *Eur. J. Immunol* 2001;31:3443–3452. [PubMed: 11745363]
- Joshi NS, Cui W, Chandele A, Lee HK, Urso DR, Hagman J, Gapin L, Kaech SM. Inflammation directs memory precursor and short-lived effector CD8⁺ T cell fates via the graded expression of T-bet transcription factor. *Immunity* 2007;27:281–295. [PubMed: 17723218]
- Sarkar S, Kalia V, Haining WN, Konieczny BT, Subramaniam S, Ahmed R. Functional and genomic profiling of effector CD8 T cell subsets with distinct memory fates. *J. Exp. Med* 2008;205:625–640. [PubMed: 18316415]
- Kaech SM, Wherry EJ. Heterogeneity and cell-fate decisions in effector and memory CD8⁺ T cell differentiation during viral infection. *Immunity* 2007;27:393–405. [PubMed: 17892848]
- Seder RA, Ahmed R. Similarities and differences in CD4⁺ and CD8⁺ effector and memory T cell generation. *Nat. Immunol* 2003;4:835–842. [PubMed: 12942084]
- Schluns KS, Lefrancois L. Cytokine control of memory T-cell development and survival. *Nat. Rev. Immunol* 2003;3:269–279. [PubMed: 12669018]
- Becker TC, Wherry EJ, Boone D, Murali-Krishna K, Antia R, Ma A, Ahmed R. Interleukin 15 is required for proliferative renewal of virus-specific memory CD8 T cells. *J. Exp. Med* 2002;195:1541–1548. [PubMed: 12070282]

14. Goldrath AW, Sivakumar PV, Glaccum M, Kennedy MK, Bevan MJ, Benoist C, Mathis D, Butz EA. Cytokine requirements for acute and basal homeostatic proliferation of naive and memory CD8⁺ T cells. *J. Exp. Med* 2002;195:1515–1522. [PubMed: 12070279]
15. Gramaglia I, Jember A, Pippig SD, Weinberg AD, Killeen N, Croft M. The OX40 costimulatory receptor determines the development of CD4 memory by regulating primary clonal expansion. *J. Immunol* 2000;165:3043–3050. [PubMed: 10975814]
16. Rogers PR, Song J, Gramaglia I, Killeen N, Croft M. OX40 promotes Bcl-x_L and Bcl-2 expression and is essential for long-term survival of CD4 T cells. *Immunity* 2001;15:445–455. [PubMed: 11567634]
17. Bertram EM, Lau P, Watts TH. Temporal segregation of 4-1BB versus CD28-mediated costimulation: 4-1BB ligand influences T cell numbers late in the primary response and regulates the size of the T cell memory response following influenza infection. *J. Immunol* 2002;168:3777–3785. [PubMed: 11937529]
18. Hendriks J, Gravestien LA, Tesselaar K, van Lier RA, Schumacher TN, Borst J. CD27 is required for generation and long-term maintenance of T cell immunity. *Nat. Immunol* 2000;1:433–440. [PubMed: 11062504]
19. Hendriks J, Xiao Y, Rossen JW, van der Sluijs KF, Sugamura K, Ishii N, Borst J. During viral infection of the respiratory tract, CD27, 4-1BB, and OX40 collectively determine formation of CD8⁺ memory T cells and their capacity for secondary expansion. *J. Immunol* 2005;175:1665–1676. [PubMed: 16034107]
20. Maxwell JR, Weinberg A, Prell RA, Vella AT. Danger and OX40 receptor signaling synergize to enhance memory T cell survival by inhibiting peripheral deletion. *J. Immunol* 2000;164:107–112. [PubMed: 10605000]
21. Murata K, Ishii N, Takano H, Miura S, Ndhlovu LC, Nose M, Noda T, Sugamura K. Impairment of antigen-presenting cell function in mice lacking expression of OX40 ligand. *J. Exp. Med* 2000;191:365–374. [PubMed: 10637280]
22. Song J, So T, Cheng M, Tang X, Croft M. Sustained survivin expression from OX40 costimulatory signals drives T cell clonal expansion. *Immunity* 2005;22:621–631. [PubMed: 15894279]
23. Croft M. Co-stimulatory members of the TNFR family: keys to effective T-cell immunity? *Nat. Rev. Immunol* 2003;3:609–620. [PubMed: 12974476]
24. Sugamura K, Ishii N, Weinberg AD. Therapeutic targeting of the effector T-cell co-stimulatory molecule OX40. *Nat. Rev. Immunol* 2004;4:420–431. [PubMed: 15173831]
25. Lee SW, Park Y, Song A, Cheroutre H, Kwon BS, Croft M. Functional dichotomy between OX40 and 4-1BB in modulating effector CD8 T cell responses. *J. Immunol* 2006;177:4464–4472. [PubMed: 16982882]
26. Song A, Tang X, Harms KM, Croft M. OX40 and Bcl-x_L promote the persistence of CD8 T cells to recall tumor-associated antigen. *J. Immunol* 2005;175:3534–3541. [PubMed: 16148096]
27. Redmond WL, Gough MJ, Charbonneau B, Ratliff TL, Weinberg AD. Defects in the acquisition of CD8 T cell effector function after priming with tumor or soluble antigen can be overcome by the addition of an OX40 agonist. *J. Immunol* 2007;179:7244–7253. [PubMed: 18025166]
28. Pope C, Kim SK, Marzo A, Masopust D, Williams K, Jiang J, Shen H, Lefrancois L. Organ-specific regulation of the CD8 T cell response to *Listeria monocytogenes* infection. *J. Immunol* 2001;166:3402–3409. [PubMed: 11207297]
29. Clarke SR, Barnden M, Kurts C, Carbone FR, Miller JF, Heath WR. Characterization of the ovalbumin-specific TCR transgenic line OT-I: MHC elements for positive and negative selection. *Immunol. Cell Biol* 2000;78:110–117. [PubMed: 10762410]
30. Soroosh P, Ine S, Sugamura K, Ishii N. Differential requirements for OX40 signals on generation of effector and central memory CD4⁺ T cells. *J. Immunol* 2007;179:5014–5023. [PubMed: 17911586]
31. Takeda I, Ine S, Killeen N, Ndhlovu LC, Murata K, Satomi S, Sugamura K, Ishii N. Distinct roles for the OX40-OX40 ligand interaction in regulatory and nonregulatory T cells. *J. Immunol* 2004;172:3580–3589. [PubMed: 15004159]
32. Yajima T, Nishimura H, Sad S, Shen H, Kuwano H, Yoshikai Y. A novel role of IL-15 in early activation of memory CD8⁺ CTL after reinfection. *J. Immunol* 2005;174:3590–3597. [PubMed: 15749896]

33. Ishii N, Ndhlovu LC, Murata K, Sato T, Kamanaka M, Sugamura K. OX40 (CD134) and OX40 ligand interaction plays an adjuvant role during in vivo Th2 responses. *Eur. J. Immunol* 2003;33:2372–2381. [PubMed: 12938213]
34. Chen S, Ishii N, Ine S, Ikeda S, Fujimura T, Ndhlovu LC, Soroosh P, Tada K, Harigae H, Kameoka J, et al. Regulatory T cell-like activity of Foxp3⁺ adult T cell leukemia cells. *Int. Immunol* 2006;18:269–277. [PubMed: 16361311]
35. Soroosh P, Ine S, Sugamura K, Ishii N. OX40-OX40 ligand interaction through T cell-T cell contact contributes to CD4 T cell longevity. *J. Immunol* 2006;176:5975–5987. [PubMed: 16670306]
36. Gramaglia I, Weinberg AD, Lemon M, Croft M. OX-40 ligand: a potent costimulatory molecule for sustaining primary CD4 T cell responses. *J. Immunol* 1998;161:6510–6517. [PubMed: 9862675]
37. Hand TW, Morre M, Kaech SM. Expression of IL-7 receptor α is necessary but not sufficient for the formation of memory CD8 T cells during viral infection. *Proc. Natl. Acad. Sci. USA* 2007;104:11730–11735. [PubMed: 17609371]
38. Haring JS, Jing X, Bollenbacher-Reilley J, Xue HH, Leonard WJ, Harty JT. Constitutive expression of IL-7 receptor α does not support increased expansion or prevent contraction of antigen-specific CD4 or CD8 T cells following *Listeria monocytogenes* infection. *J. Immunol* 2008;180:2855–2862. [PubMed: 18292507]
39. Watts TH. TNF/TNFR family members in costimulation of T cell responses. *Annu. Rev. Immunol* 2005;23:23–68. [PubMed: 15771565]
40. Williams MA, Tyznik AJ, Bevan MJ. Interleukin-2 signals during priming are required for secondary expansion of CD8⁺ memory T cells. *Nature* 2006;441:890–893. [PubMed: 16778891]

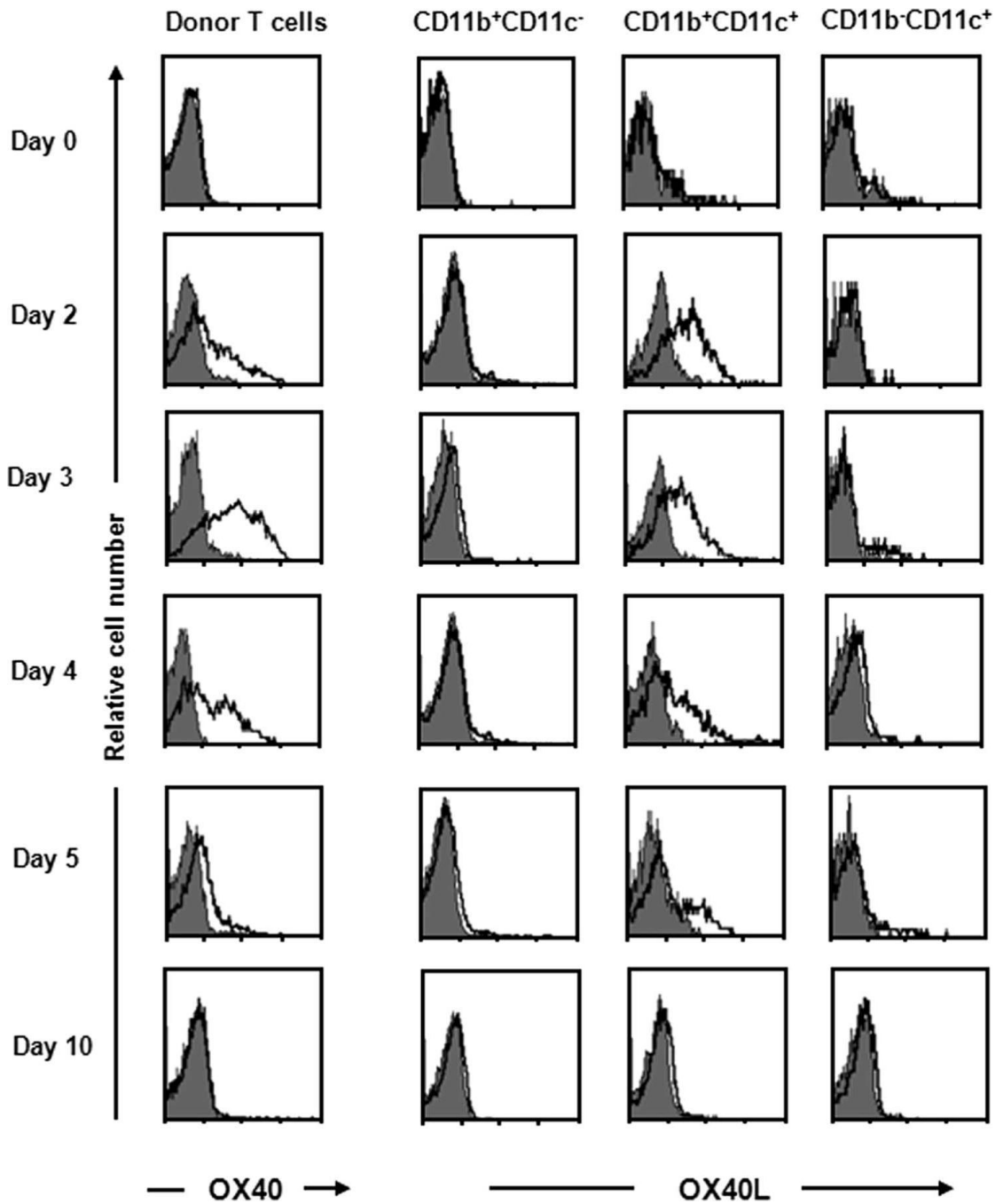
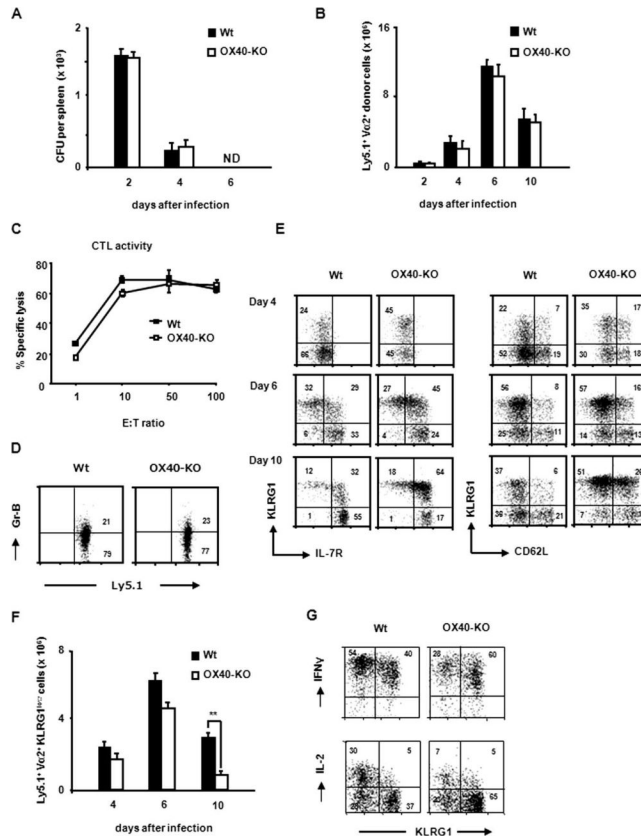


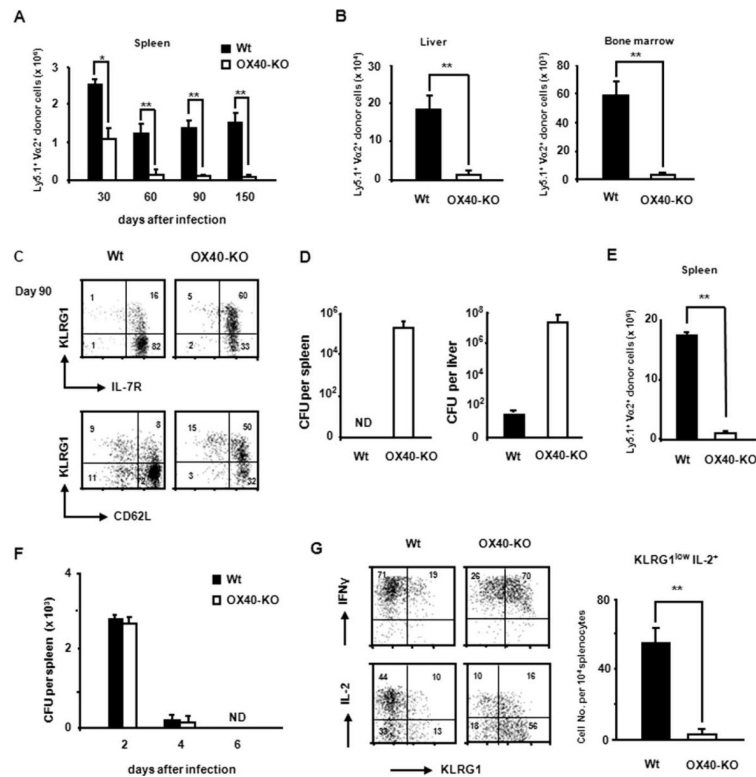
FIGURE 1.

Transient expression of OX40 and OX40L on T cells and myeloid DCs, respectively, during *rLM-OVA* infection. Purified naive Ly5.1⁺ OT-I cells (1×10^4) were adoptively transferred i.v. into Ly5.2⁺ congenic recipient mice that were infected with *rLM-OVA* (1×10^4 CFU) at 24 h after the cell transfer. The expression of OX40 on Ly5.1⁺ TCR- α 2⁺ donor cells and the expression of OX40L on recipient APCs (CD11b⁺CD11c⁻, CD11b⁺CD11c⁺, and CD11b⁻CD11c⁺) in the spleen were analyzed on the indicated days after infection. Results shown are representative mouse from each time point from one representative experiment of three.

**FIGURE 2.**

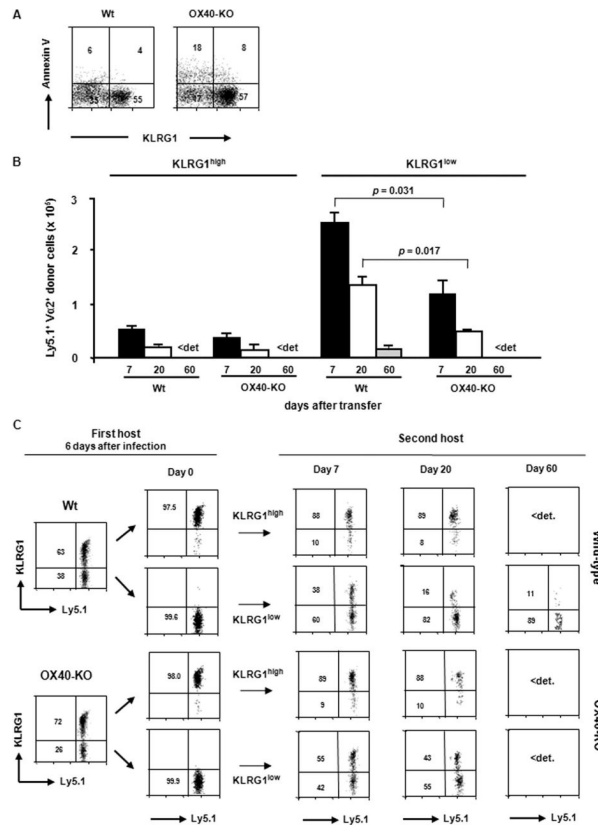
OX40 signals are dispensable for the expansion and function of activated CD8⁺ T cells, but determine the number of KLRG1^{low} MPECs. Purified naive Ly5.1⁺ OT-I or Ly5.1⁺ OX40^{-/-} OT-I cells (1×10^4 each) were adoptively transferred i.v. into Ly5.2⁺ congenic wild-type mice that were infected with rLM-OVA (1×10^4 CFU) 24 h after transfer. **A**, On the indicated days postinfection, the spleen and liver were removed and separately homogenized in PBS. Each extract was cultured in triplicate on an erythromycin-containing plate, and the erythromycin-resistant bacteria colony number was measured. The average CFU per spleen and liver from each recipient was calculated. Results represent the mean \pm SD of the average CFU from three mice per group. **B**, The absolute number of Ly5.1⁺ TCR-V α 2⁺ donor cells in the spleens of recipient mice ($n = 4$ in each group) was counted on the indicated days after infection. Results represent the mean \pm SD of the donor cell numbers from four mice per group. Similar results were obtained in two independent experiments. **C**, Spleen cells from the recipient mice ($n = 3$ each) that harbored wild-type or OX40^{-/-} OT-I cells were collected 10 days after the infection. The collected cells (effector cells) were cocultured with ⁵¹Cr-labeled EL-4 cells (4×10^4) (target cells) at the indicated ratios in the presence (10 μ g/ml) or absence of OVA₂₅₇₋₂₆₄ peptide for 6 h. After the incubation, the radioactivities of the supernatants were determined with a gamma counter. Results are the mean \pm SD of percentage of lysis obtained from three mice per group. Similar results were obtained in two independent experiments. **D**, On day 10 postinfection, intracellular granzyme B expression in wild-type OT-I and OX40^{-/-} OT-I cells from the recipient spleen was examined by flow cytometry. The number in each quadrant indicates the frequency of each subset. Results shown are representative mouse from one representative experiment of two. **E**, The kinetic expression of KLRG1 and IL-7R (left) and KLRG1 and CD62L (right) on Ly5.1⁺ wild-type OT-I or Ly5.1⁺ OX40^{-/-} OT-I donor cells was examined on the indicated days postinfection. The number in each quadrant indicates the percentage of each subset. Results shown are the

expression profiles of Ly5.1⁺ Vα2⁺ cells in pooled splenocytes from three mice, and are representative from each time point from one representative experiment of two. Similar results were obtained in two independent experiments. *F*, The absolute numbers of KLRG1^{low} cells in Ly5.1⁺ wild-type (■) and OX40^{-/-} (□) OT-I donor cells were counted on the indicated days infection. Results represent the mean ± SD of the donor cell number from four mice per group. Similar results were obtained in two independent experiments. *G*, Whole splenocytes from the recipient mice that harbored either wild-type or OX40^{-/-} OT-I cells were collected on day 10 after rLM-OVA infection, and in vitro restimulated with OVA₂₅₇₋₂₆₄ peptide for 4 h. IFN-γ and IL-2 production by KLRG1^{high} and KLRG1^{low} subsets in Ly5.1⁺ donor cells was analyzed by using intracellular staining. The number in each quadrant indicates the percentage of frequency of each subset in the Ly5.1⁺ donor cells. Similar results were obtained in two independent experiments.

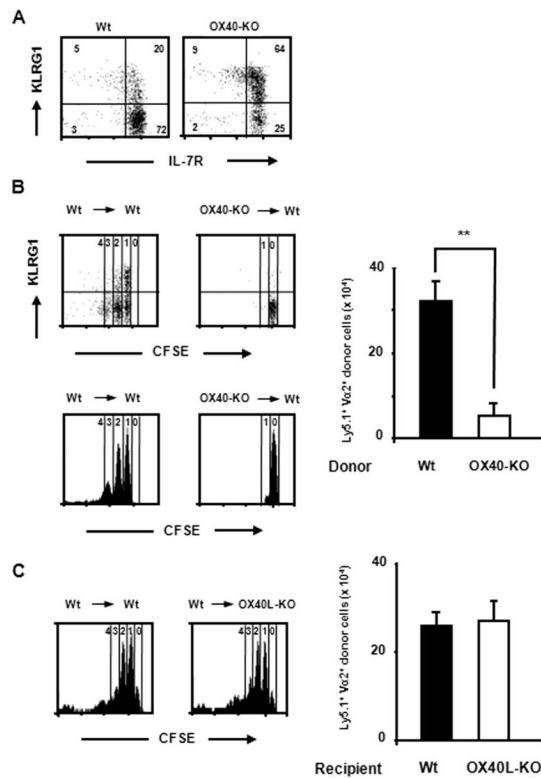
**FIGURE 3.**

OX40 signals are essential for the generation of functional memory CD8⁺ T cells. Persisting wild-type or OX40^{-/-} donor T cells, which were generated in the first host during *Listeria* infection, were tracked during memory phase. **A**, Purified naive Ly5.1⁺ OT-I or Ly5.1⁺ OX40^{-/-} OT-I cells (1×10^4 each) were adoptively transferred i.v. into Ly5.2⁺ congenic wild-type mice that were infected with rLM-OVA (1×10^4 CFU) 24 h after transfer. The absolute number of Ly5.1⁺TCR-V α 2⁺ donor cells in the spleens of recipient mice was counted on the indicated days after the infection. Results represent the mean \pm SD of the donor cell numbers from four mice per group. Similar results were obtained in two independent experiments. **B**, The absolute number of donor cells in the liver (*left*) and bone marrow (*right*) of the recipient mice was measured on day 150 after infection. Results represent the mean \pm SD from four mice per group. **C**, The expression of KLRG1 and IL-7R (*upper*), and KLRG1 and CD62L (*lower*) on Ly5.1⁺ long-lived OT-I or OX40^{-/-} OT-I cells in the spleen of the recipient mice on day 90 after infection was examined. Results are representative of four mice in each group. Similar results were obtained in the four mice in each group. **D**, On day 90 postinfection, the recipient mice ($n = 3$ in each group), which harbored either wild-type or OX40^{-/-} donor cells, were rechallenged with a higher dose of rLM-OVA (1×10^5 CFU). The spleen and liver were removed 3 days after the second infection, and separately homogenized in PBS. Each extract was cultured in triplicate on an erythromycin-containing plate, and the erythromycin-resistant bacteria colony number was measured. The average CFU per spleen and liver from each recipient were calculated. Results represent the mean \pm SD of the average CFU from three mice per group. **E**, On day 90 postinfection, the recipient mice ($n = 4$ in each group) were rechallenged with rLM-OVA (1×10^5 CFU), and the number of Ly5.1⁺TCR-V α 2⁺ donor OT-I cells in the spleens was examined 5 days after rechallenge. Results represent the mean \pm SD of the donor cell numbers from four mice in each group. Similar results were obtained in two independent experiments. **F**, The long-lived Ly5.1⁺ wild-type or OX40^{-/-} donor cells (5×10^4) generated in the first hosts were collected 45 days after infection, and transferred into the naive second recipients. The second hosts were infected with a higher dose of rLM-OVA ($1 \times$

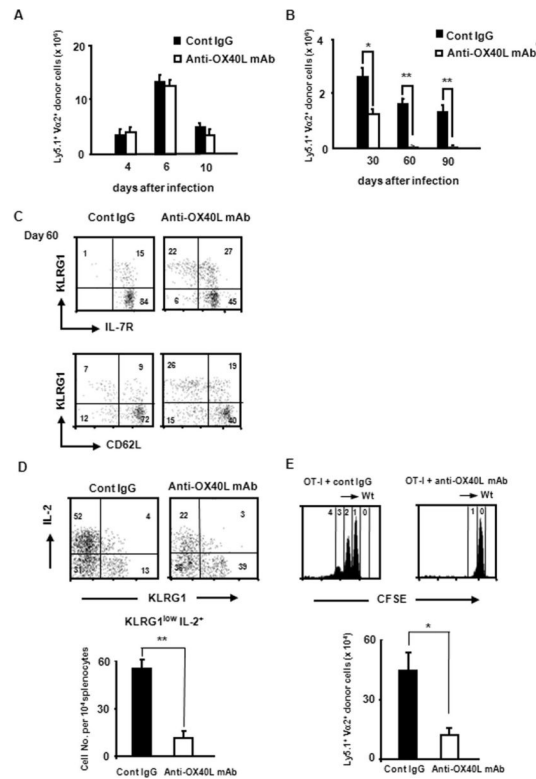
10^5 CFU), and the bacterial burden in the spleen of each group was counted at days 2, 4, and 6 of infection. Results represent the mean \pm SD of the average CFU from three mice per group. G, Production of IL-2 and IFN- γ by donor cells upon in vitro recall responses was examined, as described in Fig. 2G, on day 90 after infection. The absolute number of IL-2-producing KLRG1^{low} donor cells in the culture was counted. The number in each quadrant of the dot plots indicates percentage of frequency of each subset in the Ly5.1⁺ donor cells. Results in the dot plots are representative of three mice in each group. The graph represents the mean \pm SD of the number of IL-2-producing KLRG1^{low} donor cells per 10^4 whole splenocytes from three mice in each group. Similar results were obtained in two independent experiments.

**FIGURE 4.**

OX40 signals promote the survival of KLRG1^{low} memory precursor cells. **A**, Splens were removed from the recipient mice that harbored wild-type or OX40^{-/-} donor cells 6 days after the rLM-OVA infection. Whole splenocytes (5×10^5) that included effector donor T cells were cultured for 8 h in complete medium. The cells were then harvested and stained with anti-Ly5.1 mAb, anti-KLRG1 mAb, and annexin V. The intensity of the annexin V staining on the Ly5.1-gated cells was measured with a FACSCalibur flow cytometer. The number in each quadrant indicates the percentage of frequency of each subset in the Ly5.1⁺ donor cells. Results shown are representative mouse from each time point from one representative experiment of two. **B**, Ly5.1⁺ effector donor cells were isolated from the spleen of the first host (Ly5.2⁺) 6 days after the rLM-OVA infection with an AutoMACS cell sorter. The enriched Ly5.1⁺ donor cells were further separated by a FACSaria cell sorter to purify KLRG1^{low}TCR-Vα2⁺CD8⁺ and KLRG1^{high}TCR-Vα2⁺CD8⁺ effector T cells. These cells (2×10^6 each), from the first host, which harbored either the wild-type OT-I or OX40^{-/-} OT-I donor cells, were adoptively transferred into an Ly5.2⁺ second host (wild-type mouse) that had been infected with wild-type *L. monocytogenes* 6 days previously. The absolute number of the live Ly5.1⁺TCR-Vα2⁺ cells derived from each population in the spleen of each recipient was counted on the indicated days after transfer. The graph represents the mean \pm SD of the number of the donor cells from three mice on each day in each group. Similar results were obtained in two independent experiments. <det., Below detection. **C**, Expression of KLRG1 on Ly5.1⁺TCR-Vα2⁺ donor cells was examined on the indicated days after transfer. Results shown are representative mouse from each time point from one representative experiment of two. Similar results were obtained in the two experiments. <det., Below detection.

**FIGURE 5.**

OX40 is essential for the self-renewal potential of memory CD8⁺ T cells. Long-lived Ly5.1⁺ donor cells from the first host were transferred into Ag-naive second host, and their homeostatic proliferation was assessed. **A**, Ly5.1⁺ donor cells in the first host, which possessed either wild-type or OX40^{-/-} donor cells, were collected 40 days after infection by using an AutoMACS cell sorter. Before being transferred into second host, the donor cells were stained with anti-KLRG1 and IL-7R mAbs, and their expression profiles of KLRG1 and IL-7R were examined. The data shown are representative of independent four or five donor cell samples in each group. **B**, The purified long-lived Ly5.1⁺ donor cells from the first host were labeled with CFSE and transferred (1×10^6 in each group) into wild-type congenic mice ($n = 3$). The dilution of CFSE intensity of Ly5.1⁺TCR-Vα2⁺ donor cells in the spleen of recipient mice was assessed by flow cytometry. The absolute number of Ly5.1⁺TCR-Vα2⁺ donor cells in the spleen of the second host was counted. The data shown in the flow cytometric analysis are representative of three mice per each group. The graph represents the mean \pm SD of the absolute numbers of the donor T cells in the spleen of recipient mice ($n = 3$ in each group) on day 30 posttransfer. Similar results were obtained in two independent experiments. **C**, CFSE-labeled wild-type long-lived donor T cells (1×10^6) were transferred into naive Ly5.2⁺ congenic wild-type or OX40L^{-/-} mice ($n = 3$ each), as described above. Cell division of the donor cells in the spleen of the second host was assessed by a CFSE dilution assay. The data shown in the flow cytometric analysis are representative of three mice per each group in one representative experiment of two. The graph represents the mean \pm SD of the donor cell numbers in the spleen from recipient mice ($n = 3$ in each group) at day 30 posttransfer.

**FIGURE 6.**

Blocking of OX40 signals during priming suppresses both the generation and the maintenance of memory CD8⁺ T cells. Purified naive Ly5.1⁺ OT-I cells (1×10^4) were adoptively transferred i.v. into Ly5.2⁺ congenic recipient mice that were infected with rLM-OVA (1×10^4 CFU) at 24 h after the cell transfer. To block the OX40-OX40L interaction, the recipient mice were given control rat IgG (300 μ g) or blocking anti-OX40L mAb (MGP34) (300 μ g) by i.p. injection 1 day before, and on days 1, 3, 5, and 7 after the infection. Accumulation of effector (A) and memory (B) donor cells was determined by tracking Ly5.1⁺ TCR-V α 2⁺ cells in the spleen of each recipient mice ($n = 3$ or 4 in each group). Results represent the mean \pm SD of the absolute numbers of the donor cells in the spleens from three or four mice in each group on the indicated days, and are representative of two independent experiments. C, On day 60 postinfection, IL-7R and CD62L expression by KLRG1^{high} and KLRG1^{low} donor cells in the spleen of the recipient mice that were treated with control rat IgG or blocking anti-OX40L mAb during priming were examined by flow cytometric analysis. Results shown are representative mouse from three mice from one representative experiment of two. D, Production of IL-2 and IFN- γ by donor cells upon in vitro recall stimulation was examined on day 60 after infection, as described in Fig. 2G. The number in each quadrant of the dot plots indicates percentage of frequency of each subset in the Ly5.1⁺ donor cells. Results in the dot plots are representative of four mice in each group. The graph represents the mean \pm SD of the number of IL-2-producing KLRG1^{low} donor cells per 10⁴ whole splenocytes from four mice in each group. Similar results were obtained in two independent experiments. E, Forty days after infection, Ly5.1⁺ donor cells were purified from the first host that had been treated with anti-OX40L blocking mAb or control rat IgG (300 μ g/mouse), as described above. The purified Ly5.1⁺ donor cells (1×10^6) were transferred into Ag-naive second host, and their homeostatic proliferation was assessed 30 days after the transfer by a CFSE dilution assay, as described in Fig. 5B. The data shown in the flow cytometric analysis are representative of three mice per each group in one representative experiment of two. The graph represents the mean \pm SD of the absolute numbers

of Ly5.1⁺TCR-V α 2⁺ donor T cells in the spleen from three mice in each group at day 30 posttransfer. Similar results were obtained in two independent experiments.